Low-temperature preparation and microwave photocatalytic activity study of TiO$_2$-mounted activated carbon

Yazi Liu, Shaogui Yang, Jun Hong, Cheng Sun[*]

State Key Laboratory of Pollution Control and Resource Reuse, School of the Environment, Nanjing University, Nanjing 210093, PR China

Abstract

TiO$_2$ thin films were deposited on granular activated carbon by a dip-coating method at low temperature (373 K), using microwave radiation to enhance the crystallization of titania nanoparticles. Uniform and continuous anatase titania films were deposited on the surface of activated carbon. BET surface area of TiO$_2$-mounted activated carbon (TiO$_2$/AC) decreased a little in comparison with activated carbon. TiO$_2$/AC possessed strong optical absorption capacity with a band gap absorption edge around 360 nm. The photocatalytic activity did not increase when the as-synthesized TiO$_2$/AC was thermally treated, but was much higher than commercial P-25 in degradation of phenol by irradiation of electrodeless discharge lamps (EDLs).
© 2006 Elsevier B.V. All rights reserved.

Keywords: TiO$_2$/AC; Activated carbon; Phenol; Microwave; Photocatalytic degradation

1. Introduction

Titanium dioxide has been proved to be a very efficient photocatalyst for the degradation of biorefractory contaminants [1,2] and has been extensively used in a great variety of applications. Many works were focused on the preparation as well as on the modification of TiO$_2$ to improve its photoactivity. Large surface area and high degree of dispersion of TiO$_2$ powders in the reaction media were reported to be favorable for high photocatalytic performance. Other factors, such as preparation process, crystallinity and anatase–rutile ratio in the catalyst, are also pointed out to be important [3–5]. Adding activated carbon to TiO$_2$ can possibly increase its photocatalytic efficiency because of the large surface area of the whole composite catalyst, in which activated carbon can act as an efficient adsorption trap to the organic pollutant, which is then more efficiently transferred to TiO$_2$ surface, where it is immediately photocatalytically degraded [6].

There are many methods of producing TiO$_2$ thin films, such as sol–gel methods [7], electrochemical deposition [8], chemical vapor deposition (CVD) [9]. These methods usually require a high amount of energy and for the first two methods, an annealing post-treatment is necessary to induce the adhesion of titania to the substrate and also to enhance crystallinity and growth of the particles, which often leads to the agglomeration of anatase nanoparticles with bulk properties. Recently, various low-temperature methods for fabrication of crystalline thin films of semiconductors are receiving more and more attention, not only from the point of view of energy saving, but also allowing the use of low thermally resistant materials such as wood, carbon, paper as substrates. As for film deposition methods, Yoshimura [10] argues in favor of soft-solution processing for advanced inorganic materials for fabrication in aqueous solutions without firing, sintering or melting and using low temperatures.

The phenomenon of electrodeless discharge lamps (EDLs) generating ultraviolet–visible light when irradiated by electromagnetic field was covered by numerous patents and papers [11,12]. MW photocatalytic degradation using EDLs had received increasing interests in photochemical reactions in recent years. Klán et al. [13–18] studied the photoreduction of acetophenone, photolysis of a phenacyl ester, etc., by modified domestic MW oven integrated EDLs and found that it was possible for photodegradation of environmentally unwanted compounds as its reasonable photochemical efficiency and other advantages. MW photocatalytic degradation was superior for its simple device, simultaneous effects of UV–vis

* Corresponding author. Tel.: +86 25 83593372; fax: +86 25 83707304.
E-mail addresses: yangdlut@126.com (S. Yang), envidean@nju.edu.cn, chengsun@public1.ptt.js.cn (C. Sun).

light and MW electromagnetic radiation and EDLs in wireless way.

The aim of the present study is to explore a new soft-solution processing method in which crystallization of titania colloid is enhanced by microwave heating and TiO$_2$ thin films are deposited on activated carbon with relative ease and at low temperature. In addition, the photocatalytic activity of this composite catalyst TiO$_2$/AC was assessed by performing MW photocatalytic degradation of phenol in aqueous solutions.

2. Experimental

2.1. Materials

Phenol (AR, Tianjin Chemical Company, PR China) was chosen as the model pollutant. Tetrabutyl orthotitanate (Ti(OBu)$_4$; CP, Shanghai), absolute ethanol (EtOH; AR, Nanjing), and tetrabutylammonium hydroxide ((TBA)OH; 10% in water, Shanghai) were utilized for the synthesis of TiO$_2$ catalysts.

The same high purity granular activated carbon (Nanjing Forestry and Chemistry Research Institute, coconut shell, <1% ash) has a particle size in the range from 0.355 to 0.900 mm. The double distilled water was used in all experiments.

2.2. Preparation of TiO$_2$ thin films deposited on activated carbon

2.2.1. Pretreatment of activated carbon

Adding 10.0 g activated carbon into the boiled water with uniformly stirring for 5 min and was then ultrasonically cleaned for 30 min. After that, activated carbon was immersed into the dilute hydrochloric acid with the concentration of 7%, agitated and remained overnight. Twenty-four hours later, clear activated carbon granular was obtained by filtering and washing with distilled water repeatedly until the pH value of the filtrate was around 7. Finally, activated carbon was dried at 373 K for 5 h and stored in a desiccator for further use.

2.2.2. Preparation of titania sol

Anatase nanocrystals were prepared by the controlled hydrolysis of Ti(OBu)$_4$, using MW radiation treatment to enhance the growth of these nanoparticles. Ti(OBu)$_4$ (5 ml) was dissolved in absolute EtOH (30 ml), and the solution was added to a solution of 2.4 ml of (TBA)OH (10% in water) in 30 ml of absolute EtOH. Both solutions were preserved from atmosphere moisture before their mixture. The whole mixture was then vigorously stirred for 1 h. Afterward, 185 ml of water was added dropwise to the mixed solution and kept stirring for another 1 h to ensure the complete hydrolysis of Ti(OBu)$_4$. The obtained transparent solution, with a Ti:TBA ratio of 16:1, was heated to evaporate alcohol and other possible organics until the volume of the solution was reduced to ca. 100 ml. The solution was then heated to reflux for 1.5 h by means of a microwave furnace (Midea PJ23C-SC1) working at its lowest power level (around 150 W). After this treatment, a transparent slightly blue-colored colloidal solution was recovered, with the molar concentration of Ti^{4+} 0.15 mol/l. To gain further knowledge, non-MW-treated solutions of 30 ml,

although not used in deposition experiments, were also studied for its crystallinity. Both solid samples for powder XRD characterization were obtained from aliquots dried at 333 K.

2.2.3. Preparation of TiO$_2$ thin films

For film preparation, the dip-coating method was employed. Firstly, 5.0 g of clear activated carbon after being pretreated was immersed for 5 min into 46.4 ml of the newly prepared colloidal solution. Then, the activated carbon immersed in the solution was sonicated for 30 min to promote its adequate and uniform mixing. Afterward, the mixture was placed into the drying oven for 7–8 h at 373 K. Finally, the composite catalyst was completed with a white layer on the surface of activated carbon. After weighing the mass difference of activated carbon before deposition and after deposition, the mass percentage of loaded TiO$_2$ was 7.98%. Films so obtained were well adhered. TiO$_2$ layers on activated carbon could be thickened by means of consecutive dip-coating process.

2.3. Characterization techniques

Several techniques were used for characterization of the samples. Powder X-ray diffraction analysis (XRD) was carried out using Cu Kα radiation in a X'TRA diffractometer made in ARL Company in Swiss. Scanning electron micrograph (SEM) was performed using X650 made in Japan, Hitachi Company. Measurement of BET surface area was performed using N$_2$ adsorption/desorption isotherms on a Micromeritics ASAP 2020, and the pore size distribution (BJH method) [19] was calculated from the desorption branch. Fourier transform infrared spectra (FTIR) of TiO$_2$ nanocrystallites onto AC was recorded in a NEXUS 870 FT-IR, made in U.S. NICOLET Company. Optical absorption spectra (UV–vis) of the solid materials was recorded in the absorption mode using SHIMADZU UV-2401 UV-Vis spectrophotometer equipped with an integrating sphere attachment.

2.4. MW photoreactor and light source

A simple device is devised based on a modified domestic microwave oven that incorporates an electrodeless discharge lamp (EDL) encased in the reactor vessel to photodegrade environmental pollutants in aqueous media. Fig. 1 illustrates the schematic diagram of the batch-scale MW photochemicals reactor used in the study. The MW oven (33 cm × 33 cm × 20 cm; 900 W maximal MW output; Midea Co. Ltd.) was modified by making a port at the oven top for a condensed tube. A flat-bottom flask made of pyrex (250 ml) was placed onto the aluminum cylinder and connected with a communication pipe, which was equipped with a 60 cm-long water reflux condenser. An external aluminum tube attached to the hole of oven top was 10 cm long and has the same diameter as the port to eliminate MW leaking. The limit on the safe stray leakage of MW power density was kept below 0.5 mW/cm^2 at 2450 MHz measured at 20 cm distance from the port. EDLs (made by Nanhai Co. in China, 10 mm × 90 mm) were made of quartz and contained mercury and Ar introduced as a purge gas after bringing the
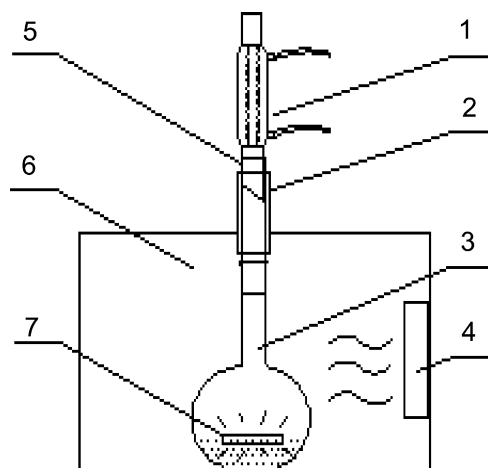
Fig. 1. Experimental set-up: (1) water reflux condenser; (2) aluminum tube; (3) flat-bottom flask; (4) MW generator; (5) communication pipe; (6) MW oven; (7) EDLs.

system to 2.7 kPa. EDLs irradiated by MW mainly emits ultraviolet and visible light wavelengths at 254, 297, 313, 366, 406, 436, 547 and 579 nm according to Klán and co-workers report [17].

The performance of this relatively simple experimental reactor was evaluated by examining the degradation of phenol using the following three techniques: (1) microwave irradiation of the phenol solution in the absence of any catalyst (blank experiment, MW); (2) photodegradation with the EDL UV–vis light excited by microwave irradiation in the absence of any catalyst, that is, MW direct photolysis (MWDP); (3) photocatalytic degradation using as-synthesized TiO_2/AC irradiated with the EDL UV–vis light excited by microwave radiation, that is, MW photocatalytic degradation (MWPD).

2.5. Procedure of MW photocatalytic degradation process

The photocatalytic test-reaction chosen to characterize the newly prepared TiO_2/AC composite catalyst was the total degra-dation of phenol, which is a well-known example of aromatic pollutant removal. All the experiments were carried out using the above batch MW photoreactor under the following conditions: the initial concentration of phenol solution was 10 mg/l with the volume of 50 ml; catalyst dosage of 2 g/l; continuously stirring; no airflow. The maximal MW power of 900 W was chosen and the stirring speed was adjusted. Reactions were performed at atmospheric pressure. UV-light was provided by an EDL excited by MW magnetic field. Samples of the suspension (10 ml) were drawn at regular intervals and immediately centrifuged by Heraeus centrifuge (Biofuge stratos, Kendro Laboratory Products) at 15 °C, 15,000 rpm for 20 min to remove catalyst particles and finally the supernatant fluid was collected and filtered through Millipore filters (0.45 μm diameter) for analysis. The concentration of phenol was determined using UV-1600 spectrophotometer at wavelength $\lambda = 270$ nm, quantitatively.

TiO_2/AC prepared in this study (0.1 g) was added under oscillating movement in 50 ml of an initial concentration of phenol (10 mg/l) and maintained in the dark for 90 min. It has been shown that this period was sufficient to reach the adsorption equilibrium. At time $t = 90$ min, the catalysts were sedimented through filtration and added to the reactor for phenol degradation.

3. Results and discussion

3.1. Characterization of TiO_2/AC composite catalyst

3.1.1. Crystal structure

X-ray diffraction was used to investigate the changes of phase structure at activated carbon before and after deposition with TiO_2. Fig. 2 depicts the XRD patterns of neat activated carbon as support and TiO_2 thin films deposited activated carbon, shown in (a) and (b), respectively. In Fig. 2(b), very broad peaks are observed at values of 2θ equal to 25.4° and 37.9° that correspond to the anatase structure. It shows that the crystal phase of films deposited on the surface of activated carbon is anatase.
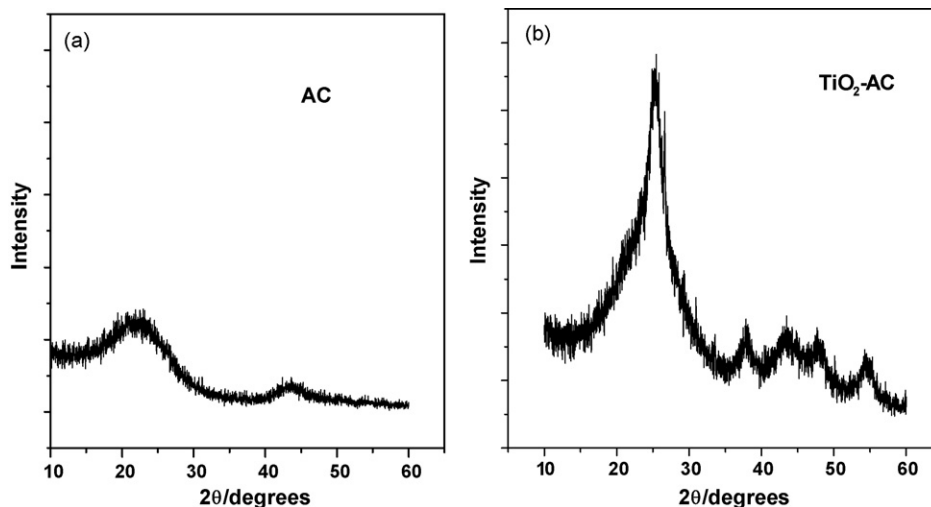

Fig. 2. X-ray diffraction patterns of: (a) neat AC; (b) AC deposited with TiO_2 films.
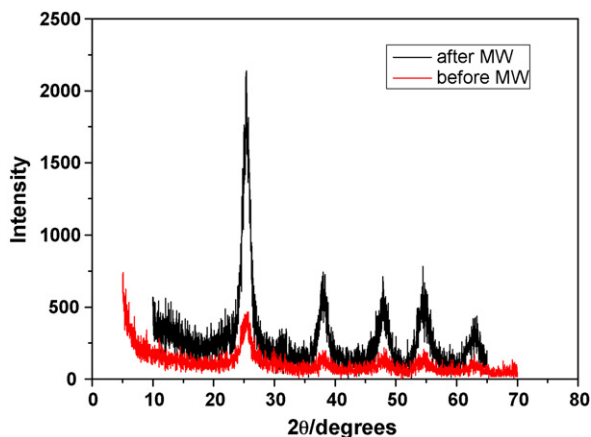
Fig. 3. X-ray diffraction pattern of TiO$_2$ crystallites obtained after evaporating the colloidal solution at 333 K after and before MW treatment, respectively.

Fig. 3 shows the XRD pattern of the TiO$_2$ crystallites obtained after evaporating the MW-treated colloidal solution used for deposition, in which broad peaks with relatively large intensity are observed at values 2θ equal to 25.6°, 38.1°, 48.2° and 54.7° that correspond to the anatase structure of titania. Furthermore, the average crystalline size calculated using the diffraction peaks [1 0 1] from Scherer's formula [20] was around 5 nm. To assess the effect of MW treatment, the crystal phase of TiO$_2$ powder recovered after evaporating the non-MW-treated colloid was also characterized. As is shown in Fig. 3, only a very broad peak with low intensities centered at 23–28° is observed. This fact suggests that non-MW-treated TiO$_2$ crystallites have a much smaller size than the MW-treated samples. MW radiation treatment proved to be an efficient way, which requires shorter time and lower temperature to enhance the growth of these particles and induce a good crystallinity.

3.1.2. SEM analysis

Activated carbon before and after deposition with TiO$_2$ films were gold-covered and examined with scanning electron microscopy (SEM) to investigate their surface morphology. The

Table 1
BET surface area and pore parameters of AC and TiO$_2$/AC

Sample	BET (m^2/g)	Pore volume (cm^3/g)	Mean pore width (nm)
AC	850.640	0.1502	23.675
TiO$_2$/AC	800.925	0.1851	26.035

SEM photograph of activated carbon pretreated with acid is shown in Fig. 4(a), in which a lot of big pores can be observed from the photograph (magnified by 5000×). Fig. 4(b) gives the SEM photograph of activated carbon deposited with TiO$_2$ films. As is shown in Fig. 4(b), titania has formed a membrane layer on the surface of activated carbon and most of the outside ports of bulk activated carbon have been covered by the TiO$_2$ membrane. The distribution of the membrane seems to be uniform and continuous. Only few cracks can be observed at the relatively thicker parts of the membrane. This phenomenon may be ascribed to the principle that the thicker the membrane, the larger the contraction stress during the drying process, thus the easier for the cracks and defects to occur. On the contrary, at the relatively thinner parts of the membrane, the defects of the support shall transfer to the membrane, which may lead to the discontinuation of the membrane. It is reported that cracks on the membrane can be effectively reduced or eliminated by repeating coating for two to three times using TiO$_2$ colloidal solution with the concentration of 0.1 mol/l [21]. While in this study, the concentration of TiO$_2$ sol prepared just equals 0.15 mol/l. This new preparation method means quality improvement of TiO$_2$ films, lower costs, relative ease and environmental-friendly processing.

3.1.3. BET surface area and pore structure

BET surface area and pore volume, together with mean pore width of AC and TiO$_2$/AC are summarized in Table 1. The results show that before film deposition, activated carbon has a BET surface area of 850.64 m^2/g; after film deposition BET surface area of this material changes to 800.92 m^2/g (the total BET surface area of activated carbon and titania film). In Fig. 5, the pore size distributions calculated by BJH method and

(a) AC
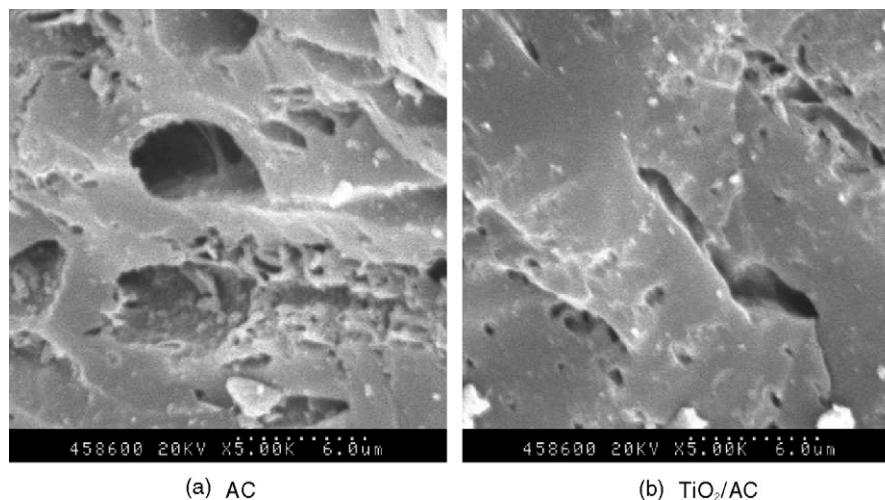

(b) TiO$_2$/AC

Fig. 4. SEM photograph of activated carbon (AC) before (a) and after (b) deposition with TiO$_2$ films.
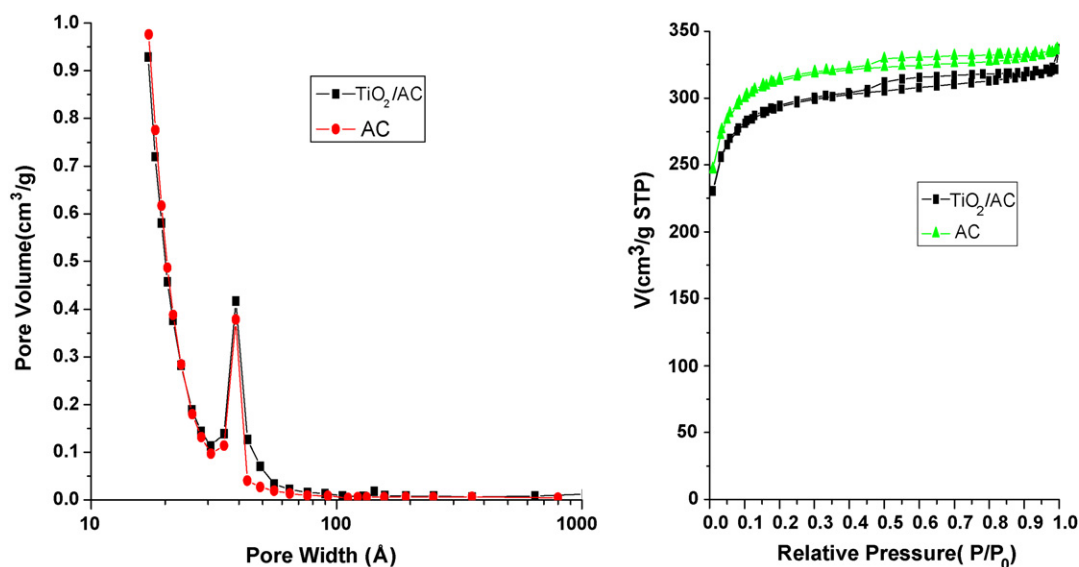
Fig. 5. N$_2$ adsorption–desorption isotherm and pore size distribution for TiO$_2$/AC and AC.

the N$_2$ adsorption–desorption isotherm were presented. Mainly mesopores were observed on both TiO$_2$/AC and AC with small amounts of micropores. The introduction of TiO$_2$ particles has led to the decrease in surface area, but the pore parameters reveal that particles of TiO$_2$ caused no obvious blocking in the mesopores of activated carbon and also no decrease in pore size. It is supposed that the decrease in surface area was caused by blocking the micropore entrances on the surface of activated carbon by TiO$_2$ particles. Since large amount of internal surface of activated carbon remained unoccupied, TiO$_2$/AC still shows very strong adsorptive capacity, which is favorable for photocatalytic reactions.

3.1.4. Optical property

The FTIR spectrum of this composite material is characterized with specific bonds corresponding to titanium in the framework, as is shown in Fig. 6. It was reported that the peak around 800 cm^{-1} is attributed to asymmetric stretching vibration of Ti–O–Ti bond, while the peaks around 1640 cm^{-1} is due to the bending vibration of O–H bond of the chemisorbed water,
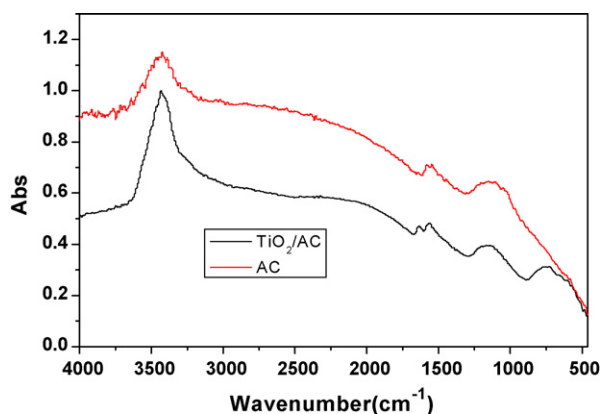
and the peaks around 3500 cm^{-1} is assigned to the stretching mode of O–H bond and is related to free water. No obvious peaks assignable to TBA cations are observed.

The UV–vis absorption spectra of the used samples (AC and TiO$_2$/AC) is given in Fig. 7. It is easily observed that for AC, the absorption is total over all range of the UV–vis spectrum with almost the same value. The TiO$_2$/AC catalytic system shows basically the same absorption pattern as the bare AC in the visible range (>400 nm) with a much lower absorption value, while in the UV range at the wavelength around 365 nm, the absorption spectra shows the typical character of titania with a band gap absorption edge around 360 nm, an obvious blue shift in the absorption edge relative to bulk anatase, which may be explained in terms of the quantum size effects that emerge in semiconductors with decreasing particle size. The optical band gap energy E_g of 3.41 eV was obtained by extrapolating to zero the linear region of the UV–vis spectra of TiO$_2$/AC, calculated according

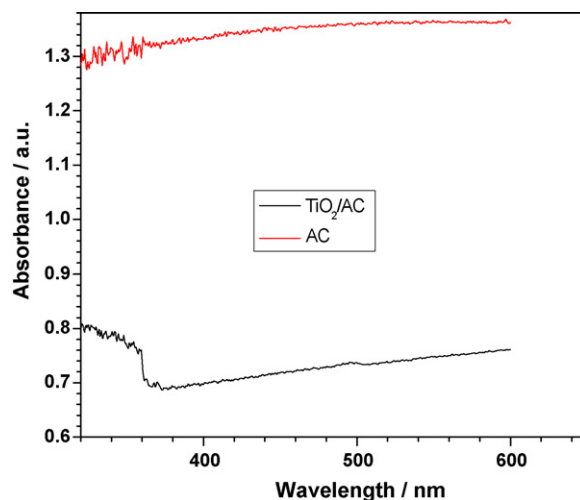Fig. 6. FTIR spectra of activated carbon (AC) and TiO$_2$-mounted activated carbon (TiO$_2$/AC).

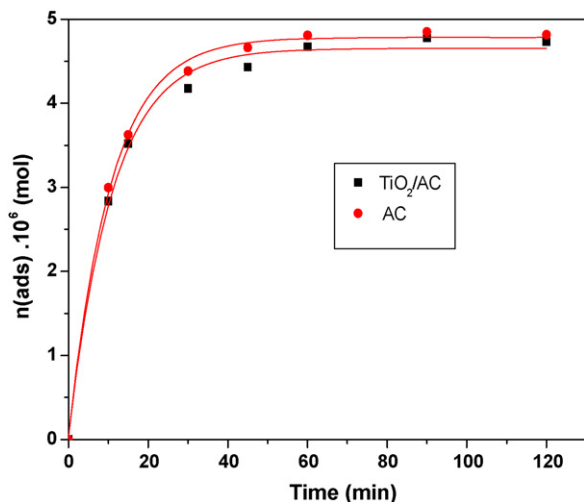Fig. 7. UV–vis absorption spectra of the activated carbon (AC) and the composite catalyst (TiO$_2$/AC).

Fig. 8. Adsorbed phenol in the dark for $C_0 = 1.06 \times 10^{-4}$ mol/l. AC (0.1 g) and TiO$_2$/AC (0.1 g).

Fig. 9. The temporal loss of phenols by the methods of MW, MWDP and MWPD. EDL-1, 2 g/l TiO$_2$/AC; 50 ml solution; 10 mg/l initial concentration of phenol; stirred; no airflow.

to Peiró et al.'s report [22]. Its light absorption intensity is relatively strong since the irradiation is carried on with the EDL light at 250–600 nm.

3.2. MW photocatalytic activity of TiO$_2$/AC composite catalyst

3.2.1. Adsorption of phenol

All batch equilibrium experiments were conducted in the dark. The study of phenol adsorption has been performed at 303 K on AC (0.1 g) and on TiO$_2$/AC (0.1 g), respectively. A pH value of about 5.3 was used. The kinetics of adsorption are given in Fig. 8 for $C_0 = 1.06 \times 10^{-4}$ mol/l (initial concentration of phenol). It can be observed that most of adsorption occurred within 60 min. The equilibrium concentration was determined using UV-1600 spectrophotometer after centrifugation and filtration, through Millipore filters (0.45 μm diameter) of the suspension. The amounts of phenol adsorbed are calculated as follows:

$$n(\text{ads}) = V\Delta C \tag{1}$$

where $n(\text{ads})$ is the number of moles adsorbed; ΔC the difference between the initial concentration, C_0 and equilibrium concentration, C_e; V is the volume (50 ml).

It can be seen from Fig. 8 that the adsorption capacity on TiO$_2$/AC is slightly smaller than on neat AC. And as both of the adsorptions gradually reach their equilibrium, the amount $n(\text{ads})$ on TiO$_2$/AC and AC get close to each other. It can be observed that TiO$_2$/AC still remains a high adsorption capacity relative to neat AC. The reason of this phenomenon can be ascribed to its unobvious decrease of surface area, which is in accordance with the BET surface area characterization results.

3.2.2. MW photocatalytic degradation of phenol

The temporal decrease of the concentration of phenol by different processes is illustrated in Fig. 9. The removal rate for phenol by the methods of MW, MWDP and MWPD reaches 7, 43 and 87%, respectively. The result shows that phenol has lit-
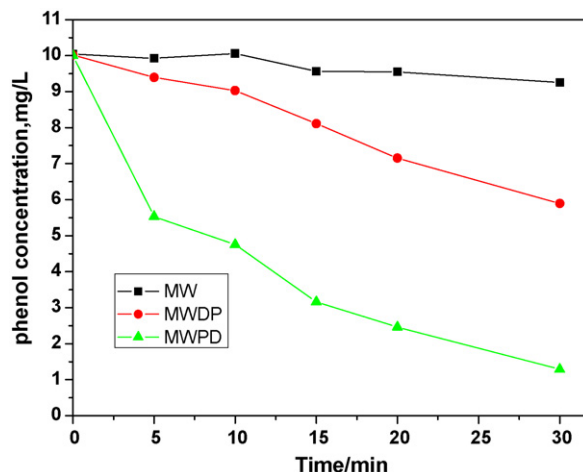
tle loss during the process of MW only. As the energy of MW ($E = 1$ J mol^{-1} at $\nu = 2450$ MHz) was insufficient to cleave most chemical bonds, the removal of phenol by MW could be ascribed to MW heating effect. As is shown in Fig. 9, the removal rate of phenol by the MWDP method is lower than by the MWPD method but higher than by the MW method. The degradation of phenol in MWDP process may be ascribed to two effects. One is the thermal effect of microwave radiation, as can be seen during the MW process alone; the other may be due to the UV–vis photodegradation provided by the EDL. As EDL excited by MW emitted wavelength from 254 to 579 nm, direct illumination of aqueous solution by EDL could generate organic activated radicals from photolysis of phenol. These radical intermediates were subsequently trapped by dissolved molecular oxygen, via the charge transfer complex (CTC), peroxyl radicals (ROO$^\bullet$), and thus induced an enhancement of the overall degradation process.

Clearly, MWPD process caused a relatively faster and effective degradation of phenol, its removal rate finally reached 87% using the TiO$_2$/AC catalyst. This indicates that TiO$_2$/AC irradiated by EDL largely accelerated the photoreactions in this specific MW assisted photoreactor. The composite TiO$_2$/AC catalyst largely reserves the excellent adsorptive capacity, which ensures an integrative process from adsorption to reaction, and to separation of reacting agents in the photocatalytic reaction system, thus leading to the enhancement of photocatalytic efficiency finally [23]. There is a transfer of phenol adsorbed on activated carbon to titania where it is immediately photocatalytically degraded. The other reason may be due to the especially strong microwave absorption and light absorption capacity of TiO$_2$/AC, which can be easily activated by MW and then serve as an effective catalyst for organic pollutant degradation in MW field [24,25].

3.2.3. Comparison of photocatalytic activity

The photocatalytic activity of several catalysts towards the degradation of phenol in aqueous solutions was conducted. Fig. 10 shows the MW photocatalytic degradation (MWPD) of
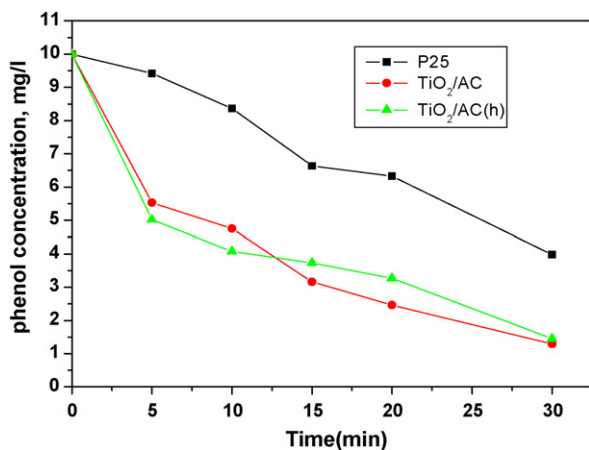
Fig. 10. Phenol removal by MWPD method using P-25, TiO$_2$/AC without thermal treatment and TiO$_2$/AC (h) with thermal treatment. EDL-1, 2 g/l catalyst; 50 ml solution; 10 mg/l initial concentration of phenol; stirred; no airflow.

phenol using the following photocatalysts: (i) P-25 (Degussa Germany) (mainly anatase with a surface area of 50 m^2/g); (ii) as-deposited TiO$_2$/AC not annealed; (iii) heat-treated TiO$_2$/AC sample at 773 K for 1 h under a flow of nitrogen, labeled as TiO$_2$/AC (h). The quantity of 2 g/l was selected as it gives a comparatively high degradation rate using commercial TiO$_2$ P-25 as a reference. The removal rate of phenol finally reached 60, 87 and 85%, respectively after irradiation of 30 min, corresponding to P-25, TiO$_2$/AC and TiO$_2$/AC (h). As for TiO$_2$/AC and P-25, the result shows that preparation of TiO$_2$/AC by microwave treatment at low temperature allows well-crystallized titania with photocatalytic activity much higher than commercial P-25. For the same catalyst dosage in the experiments, the usage of titania equals to only 0.16 g/l for composite TiO$_2$/AC catalyst with high degradation efficiency; while 2 g/l for P-25. The adding of activated carbon has dramatically increased the degradation efficiency of phenol with much lower titania concentration. As for TiO$_2$/AC and TiO$_2$/AC (h), this result shows little difference in their degradation rates. Obviously, TiO$_2$/AC (h) possesses no higher photoactivity than as-deposited TiO$_2$/AC not annealed. This fact implies that no annealing treatment is necessary in the present case to induce crystallinity in samples in order to improve photocatalytic activity, as is the general case [26]. We also found that TiO$_2$ films were well adhered with granular activated carbon with no titania entering into the reaction liquid. Adhesion was evaluated by blank experiment with water under the same conditions, after 5 min of reaction, no modification of the UV absorbance was observed, which is due to the strong adsorbability of activated carbon and also the small amount of titania deposited. The composite catalyst synthesized in this way possesses good adhesiveness and catalysis.

Several experimental results indicated that the destruction rates of photocatalytic oxidation of various organic contaminants over illuminated TiO$_2$ accord with pseudo-first-order kinetics [27–30].

$$\ln\left(\frac{C_0}{C}\right) = kKt = k_{app}t \quad \text{or} \quad C_t = C_0\,e^{-k_{app}t} \qquad (2)$$

Table 2
Apparent first-order rate constants (k_{app}) for different MW photocatalysts

MWPD photocatalysts	k_{app} (min^{-1})	R^2
TiO$_2$/AC	0.07095	0.9837
TiO$_2$/AC (h)	0.06512	0.9243
P-25	0.02692	0.9482

where C_0 is the initial concentration of the reactant; C_t the concentration of the reactant at t illumination time; t the illumination time; k the reaction rate constant; K is the adsorption coefficient of the reactant. A plot of ln C_0/C_t versus time represents a straight line, the slope of which upon linear regression equals the apparent first-order rate constant k_{app}. The apparent first-order rate constants (k_{app}) for different photocatalysts, which are calculated from Fig. 10, are presented in Table 2. k_{app} has been used as comparison parameter, since it is independent of the used concentration. It enables one to determine a photocatalytic activity independent of the previous adsorption period in the dark. The degradation rate of phenol by the TiO$_2$/AC composite catalyst was thus two-fold faster than by P-25 powder.

4. Conclusions

In summary, nanocrystalline TiO$_2$ anatase deposited on activated carbon with a method performed at low temperature shows good adherence and photocatalytic activity. Microwave radiation has proved to be a perspective technique not only for crystalline TiO$_2$ films preparation, thus allowing a wide selection of different materials as substrates, but for effective enhancement of the efficiency of photocatalytic system. Composite TiO$_2$/AC materials exhibited high photocatalytic activity for the degradation of phenol with the rate constant two-fold faster than by P-25 powder in the MW photocatalytic device.

Acknowledgments

References

[1] L. Sánchez, J. Peral, X. Domenech, Photocatalyzed destruction of aniline in UV-illuminated aqueous TiO$_2$ suspensions, Electrochim. Acta 42 (1997) 1877–1882.

[2] A. Mills, S. Le Hunte, An overview of semiconductor photocatalysis, J. Photochem. Photobiol. A: Chem. 108 (1997) 1–35.

[3] M. Inagaki, Y. Nakazawa, M. Hirano, Y. Kobayashi, M. Toyoda, Preparation of stable anatase-type TiO$_2$ and its photocatalytic performance, Int. J. Inorg. Mater. 3 (2001) 809–811.

[4] T. Tsumura, N. Kojitani, I. Izumi, N. Iwashita, M. Toyoda, M. Inagaki, Carbon coating of anatase-type TiO$_2$ and photoactivity, J. Mater. Chem. 12 (2002) 1391–1396.

[5] C.K. Chan, J.F. Porter, Y.G. Li, W. Guo, C.M. Chan, The effect of calcination on the microstructures and photocatalytic properties of nano-sized TiO$_2$ powders prepared by vapor hydrolysis, J. Am. Ceram. Soc. 82 (1999) 566–572.

[6] J. Matos, J. Laine, J.M. Herrmann, Effect of the type of activated carbons on the photocatalytic degradation of aqueous organic pollutants by UV-irradiated titania, J. Catal. 200 (2001) 10–20.

[7] (a) Å.K. Jämting, J.M. Bell, M.V. Swain, L.S. Wielunski, R. Clissold, Measurement of the micro mechanical properties of sol–gel TiO_2 films, Thin Solid Films 332 (1998) 189–194;
(b) H. Lin, H. Kozuka, T. Yoko, Preparation of TiO_2 films on self-assembled monolayers by sol–gel method, Thin Solid Films 315 (1998) 111–117;
(c) T. Nishide, F. Mizukami, Effect of ligands on crystal structures and optical properties of TiO_2 prepared by sol–gel processes, Thin Solid Films 353 (1999) 67–71.

[8] C. Natarajan, G. Nogami, Cathodic electrodeposition of nanocrystalline titanium dioxide thin films, J. Electrochem. Soc. 143 (1996) 1547–1550.

[9] J.A. Agllon, A. Figueras, S. Garelik, L. Spirkova, J. Durand, Preparation of TiO_2 powder using titanium tetraisopropoxide decomposition in a plasma enhanced chemical vapor deposition (PECVD) reactor, J. Mater. Sci. Lett. 18 (1999) 1319–1321.

[10] M. Yoshimura, Importance of soft, solution processing for advanced inorganic materials, J. Mater. Res. 13 (1998) 796–802.

[11] V. Církva, M. Hájek, Microwave photochemistry. Photoinitiated radical addition of tetrahydrofuran to perfluorohexylethene under microwave irradiation, J. Photochem. Photobiol. A: Chem. 123 (1999) 21–23.

[12] P. Klán, J. Literák, M. Hájek, The electrodeless discharge lamp: a prospective tool for photochemistry, J. Photochem. Photobiol. A: Chem. 128 (1999) 145–149.

[13] J. Literák, P. Klán, The electrodeless discharge lamp: a prospective tool for photochemistry: Part 2. Scope and limitation, J. Photochem. Photobiol. A: Chem. 137 (2000) 29–35.

[14] P. Klán, J. Literák, S. Relich, Molecular photochemical thermometers: investigation of microwave superheating effects by temperature dependent photochemical processes, J. Photochem. Photobiol. A: Chem. 143 (2001) 49–57.

[15] P. Klán, M. Hájek, V. Církva, The electrodeless discharge lamp: a prospective tool for photochemistry: Part 3. The microwave photochemistry reactor, J. Photochem. Photobiol. A: Chem. 140 (2001) 185–189.

[16] M.T. Radoiu, Y. Chen, M.C. Depew, Catalytic conversion of methane to acetylene induced by microwave irradiation, Appl. Catal. B: Environ. 43 (2003) 187–193.

[17] P. Müller, P. Klán, V. Církva, The electrodeless discharge lamp: a prospective tool for photochemistry: Part 4. Temperature- and envelope material-dependent emission characteristics, J. Photochem. Photobiol. A: Chem. 158 (2003) 1–5.

[18] J. Literák, P. Klán, D. Heger, A. Loupy, Photochemistry of alkyl aryl ketones on alumina, silica-gel and water ice surfaces, J. Photochem. Photobiol. A: Chem. 154 (2003) 155–159.

[19] E.P. Barret, L.G. Oyner, P.P. Halenda, The determination of pore volume and area distributions in porous substances. I. Computations from nitrogen isotherms, J. Am. Chem. Soc. 73 (1951) 373–380.

[20] H.P. Klug, L.E. Alexander, X-ray Diffraction Procedures, Wiley, New York, 1954.

[21] L.Q. Wu, P. Huang, N.P. Xu, et al., Preparation of supported TiO_2 ultra-filtration membranes by sol–gel technique, J. Chem. Eng. Chin. Univ. 13 (1999) 205–210.

[22] A.M. Peiró, J. Peral, C. Domingo, X. Domènech, J.A. Ayllón, Low-temperature deposition of TiO_2 thin films with photocatalytic activity from colloidal anatase aqueous solutions, Chem. Mater. 13 (2001) 2567–2573.

[23] A. Fernandez, G. Lassaletta, V.M. Jimenez, et al., Preparation and characterization of TiO_2 photocatalysts supported on various rigid supports (glass, quartz and stainless steel). Comparative studies of photocatalytic activity in water purification, Appl. Catal. B: Environ. 7 (1995) 49–63.

[24] C.H. Jou, H.S. Tai, Application of granulated activated carbon packed-bed reactor in microwave radiation field to treat BTX, Chemosphere 37 (1998) 685–698.

[25] H.S. Tai, C.H. Jou, Application of granular activated carbon packed-bed reactor in microwave radiation field to treat phenol, Chemosphere 38 (1999) 2667–2680.

[26] R.L. Pozzo, M.A. Baltanás, A.E. Cassano, Supported titanium oxide as photocatalyst in water decontamination: state of the art, Catal. Today 39 (1997) 219–321.

[27] J. Matos, J. Laine, J.M. Herrmann, Synergy effect in the photocatalytic degradation of phenol on a suspended mixture of titania and activated carbon, Appl. Catal. B 18 (1998) 281–291.

[28] R.W. Matthews, Photooxidative degradation of colored organics in water using supported catalysts. Titanium dioxide on sand, Water Res. 25 (1991) 1169–1176.

[29] T.C. An, X.H. Zhu, Y. Xiong, Feasibility study of photoelectrochemical degradation of methylene blue with three-dimensional electrode-photocatalytic reactor, Chemosphere 46 (2002) 897–903.

[30] I.K. Konstantinou, T.A. Albanis, Photocatalytic transformation of pesticides in aqueous titanium dioxide suspensions using artificial and solar light: intermediates and degradation pathways, Appl. Catal. B 42 (2003) 319–335.